Biochemical and Biophysical Research Communications 446 (2014) 441–447

Contents lists available at ScienceDirect

Biochemical and Biophysical Research Communications

journal homepage: www.elsevier.com/locate/ybbrc

Delivery of kinesin spindle protein targeting siRNA in solid lipid nanoparticles to cellular models of tumor vasculature

Bo Ying, Robert B. Campbell *

Northeastern University, Bouvé College of Health Sciences, Department of Pharmaceutical Sciences, 360 Huntington Avenue, Boston, MA 02115, United States

ARTICLE INFO

Article history:
Received 20 February 2014
Available online 4 March 2014

Keywords:
Cancer
Liposomes
Nanoparticles
Polyethyleneglycol
siRNA

ABSTRACT

The ideal siRNA delivery system should selectively deliver the construct to the target cell, avoid enzymatic degradation, and evade uptake by phagocytes. In the present study, we evaluated the importance of polyethylene glycol (PEG) on lipid-based carrier systems for encapsulating, and delivering, siRNA to tumor vessels using cellular models. Lipid nanoparticles containing different percentage of PEG were evaluated based on their physical chemical properties, density compared to water, siRNA encapsulation, toxicity, targeting efficiency and gene silencing *in vitro*. siRNA can be efficiently loaded into lipid nanoparticles (LNPs) when DOTAP is included in the formulation mixture. However, the total amount encapsulated decreased with increase in PEG content. In the presence of siRNA, the final formulations contained a mixed population of particles based on density. The major population which contains the majority of siRNA exhibited a density of 4% glucose, and the minor fraction associated with a decreased amount of siRNA had a density less than PBS. The inclusion of 10 mol% PEG resulted in a greater amount of siRNA associated with the minor fraction. Finally, when kinesin spindle protein (KSP) siRNA was encapsulated in lipid nanoparticles containing a modest amount of PEG, the proliferation of endothelial cells was inhibited due to the efficient knock down of KSP mRNA. The presence of siRNA resulted in the formation of solid lipid nanoparticles when prepared using the thin film and hydration method. LNPs with a relatively modest amount of PEG can sufficiently encapsulate siRNA, improve cellular uptake and the efficiency of gene silencing.

1. Introduction

The revolutionary finding that angiogenesis is critical for tumor growth and metastasis has created new opportunities in the fight against cancer [1]. For example, the destruction of the structure and function of tumor blood vessels, and the suppression of cancer-associated neovessel formations, are two extensively studied areas of research investigation [2]. Angiogenesis is a well-orchestrated process controlled by a variety of angiogenic promoters and inhibitors, and newly formed blood vessels may possess very different properties based on the anatomic location of the tumor and the availability of growth factors [3]. For example, angiogenic blood vessels exhibit the overexpression of *negatively charged* functional groups such as proteoglycans and glycosaminoglycans on the luminal side of the tumor vessel wall [4], permitting the more selective targeting of angiogenic vessels with cationic molecular therapeutics [4]. Studies have shown that tumor endothelial cells preferentially take up cationic liposomes rather than the electroneutral or anionic variety [5], supporting the notion that the overabundance of anionic functional groups is an exploitable tumor feature for cancer therapy [4,6].

RNA interference (RNAi) is a mechanism for RNA-guided regulation of gene expression in which double-stranded ribonucleic acid inhibits the expression of genes with complementary nucleotide sequences [7,8]. To condense DNA molecules and to enhance their uptake by cells, the first and second generation positively-charged lipids (such as stearlyamine, and DOTAP), are frequently employed for gene targeting [9–12]. In order to secure the gene silencing-potential of siRNA, the carrier molecule must be capable of delivering siRNA to target cells without cellular toxicity. Although the SNALP technology has successfully demonstrated potent siRNA delivery in pre-clinical and early stage clinical trials, SNALP process and the proprietary cationic lipids employed such as DLinDMA [13] are still not available to most of the academic labs, which makes DOTAP still the most widely used cationic lipid in research labs. As a research tool, siRNA can be easily formulated in lipid particles through conventional methods such as thin film hydration and

* Corresponding author. Address: MCPHS University, Department of Pharmaceutical Sciences, 19 Foster Street, Worcester, MA 01608-1715, United States. Fax: +1 508 373 2801.
E-mail address: robert.campbell@mcphs.edu (R.B. Campbell).

http://dx.doi.org/10.1016/j.bbrc.2014.02.120
0006-291X/

extrusion. However, little is known about the structure of lipid nanoparticles (LNPs), and whether the structure of the conventional liposomes is preserved in the presence of siRNA.

Kinesin spindle protein (KSP), a member of kinesin superfamily, plays a critical role in mitosis as it mediates the separation of centrosomes and bipolar spindle assembly [14,15]. Inhibition of KSP function will lead to the failure of centrosome segregation, prolonged cell cycle arrest at mitosis and eventually, cell death [16,17]. In contrast to microtubules which are also present in post-mitotic neurons, KSPs are exclusively expressed in mitotic cells making them an ideal target for anti-cancer therapy [15]. Therefore, since tumor endothelial cells rapidly divide, selective delivery of KSP inhibitors to vessels will result in apoptosis of endothelial cells and the suppression of tumor growth.

In the present study, we evaluated lipid-based delivery systems regarding the encapsulation capacity for siRNA, the possible structure of nanoparticles based on their density, the delivery of siRNA to cellular models of the tumor endothelium, and the efficiency of gene silencing *in vitro*.

2. Materials and methods

2.1. Materials

1,2-Dioleoyl-sn-Glycero-3-Phosphoethanolamine (DOPE), 1,2-Dioleoyl-sn-Glycero-3-Phosphocholine (DOPC), 1,2-Dioleoyl-3-Trimethylammonium-Propane (DOTAP), 1,2-Dioleoyl-sn-Glycero-3-Phosphoethanolamine-N-[Methoxy(Polyethylene glycol)-2000 (DOPE-PEG_{2000}), 1,2-dipalmitoyl-sn-glycero-3-phosphoethanolamine-N-(lissamine rhodamine B sulfonyl) (rhodamine-DPPE), 1,2-Dioleoyl-sn-Glycero-3-Phosphoethanolamine-N-(Carboxyfluorescein) (CF-DOPE) were purchased from Avanti Polar Lipids (Alabaster, AL). 1,2-Distearoyl-sn-glycerol, methoxypolyethylene Glycol 2000 (DSG-PEG_{2000}) was purchased from NOF America Corporation (White Plains, NY). Sulforhodamine B (SRB) was purchased from Sigma–Aldrich (St. Louis, MO). Cy3 labeled random sequence siRNA (MW ~13 kDa, no chemical modifications) was purchased from Applied Biosystems (Austin, TX). Ribogreen kit was purchased from Life Technologies (Grand Island, NY). KSP siRNA and control siRNA for growth inhibition studies were generously provided by Alnylam Pharmaceuticals (Cambridge, MA). RNA-Stat-60 was purchased from Tel-Test, Inc. (Friendswood, TX). Primers for KSP and beta-actin mRNA were purchased from Applied Biosystems (Austin, TX).

2.2. Cell Culture

Murine endothelial cell line MS1-VEGF and human primary umbilical vein endothelial cell line (HUVEC) were purchased from ATCC (American Type Culture Collection, Manassas, VA). Human dermal microvascular endothelial cell (HMEC-1) line was obtained from Centers for Disease Control and Prevention (Atlanta, GA). All cell line cultures were grown in a humidified atmosphere of 5% CO_2 at 37 °C.

2.3. Lipid nanoparticle preparation

The lipid nanoparticles employed for this study were classified as either DOPC (DOPC/DOTAP/DOPE-PEG_{2000}) or DOPE (DOPE/DOTAP/DOPE-PEG_{2000}) based preparations, and were used at different molar ratios (100/0/0, 50/50/0, 48/50/2, 45/50/5 and 40/50/10). The ratio between lipids and RNA is 10/1 (wt/wt). Carboxyfluorescein or rhodamine was added into LNPs at the ratio of 1 mol% if fluorescence indicators were needed. LNPs were prepared by thin film and hydration method as previously reported [5]. To reduce particle size, particles were passed through 0.1 μm filter for 11 cycles using extruders (Avanti Polar Lipids, Alabaster, AL).

2.4. Characterization of siRNA containing lipid nanoparticles

Particle size and zeta (ζ) potential of LNPs after extrusion were determined using 90 Plus Particle/Zeta Potential Analyzer (Brookhaven Instruments, Holtsville, NY). To remove free siRNA, particles were dialyzed in 50 kDa MWKO membrane against 20× volume of 1× PBS overnight. The encapsulation of siRNA was evaluated using Ribogreen assay according to manufacturer's protocol with four replicates per sample, and 0.1% triton X-100 was used to deformulate particles. The encapsulation rate was calculated as

$$\%\text{Encapsulation} = 100 - 100 * \text{MFI}_{\text{associated}}/\text{MFI}_{\text{total}}$$

Continuous glucose gradient ranging from 0 to 10 percent (w/v) was used to separate particles based on density. The gradient was prepared in an ultracentrifuge tube using a gradient maker. Empty liposomes and siRNA containing particles were loaded into different centrifuge tubes and then centrifuged at 120,000 rpm for 2 h. Particles at different density were collected and characterized based on size and siRNA content.

2.5. Uptake of formulated siRNA by cells

Cells were seeded at $5 * 10^5$ cells per ml in 6-well plates for 24 h to allow complete attachment. After being exposed to siRNA (Cy3-labeled) containing LNPs (CF-labeled) for an additional 6 h, cells were trypsinized and analyzed using flow cytometer.

2.6. Growth inhibition by KSP siRNA

Cells were seeded at $1 * 10^4$ cells per ml into 48-well plates and incubated for 24 h to allow complete attachment. KSP siRNA or control siRNA formulated with different LNPs were added to MS1-VEGF cells at increased concentrations. Sulforhodamine B assay was employed to detect the growth inhibition after 48 h of incubation.

2.7. RNA isolation and real-time RT-PCR

Cells were seeded at $5 * 10^5$ cells per ml into 6-well plates and incubated for 24 h to allow complete attachment. KSP siRNA or control siRNA formulated with different LNPs were added to MS1-VEGF cells at a fixed concentration of 100 nM. After the exposure to siRNA for 48 h, total RNA were extracted from MS1-VEGF cells using RNA-STAT-60 (TEL-TEST, Friendswood, TX) according to the manufacturer's instructions. The total RNA extracted from cells was reverse transcribed to synthesize cDNA using SuperScript® first-strand synthesis kit (Invitrogen, Carlsbad, CA). Real-time PCR was performed using Taqman master mix (Applied Biosystems, Foster City, CA). Beta-actin mRNA was employed as the internal standard. The real-time PCR was performed using Applied Biosystems 7300 Real-Time PCR system (Foster City, CA).

2.8. Statistics

Unless mentioned specifically, data were analyzed in SPSS 16.0 using One-Way ANOVA, post hoc Tukey, and plotted using Sigmaplot 11.0 (Systat Software, Inc., San Jose, CA). In the present study, the following were used as measurements of statistical significance, $^{*}p < 0.05$; $^{**}p < 0.01$; $^{***}p < 0.001$.

3. Results

3.1. Characterization of lipid nanoparticles

Particle size and zeta (ζ) potential of lipid nanoparticles (LNPs) were determined using 90 Plus Particle/Zeta Potential Analyzer (Table 1). In the DOPC based formulation group, the particle size decreased significantly from 178 to 149 nm following the inclusion of DOTAP. The inclusion of 2 mol% of DOPE-PEG_{2000} N Engl J Medfurther reduced the particle size to 113 nm. An additional increase in the amount of PEG did not alter LNP size. Particles formed by DOPC alone exhibited zeta potential of 2 mV. The incorporation of 50 mol% of DOTAP significantly increased the zeta potential to 45 mV. When 2, 5 and 10 mol% of PEG was incorporated into DOPC/DOTAP particles, the zeta potential decreased to 34, 23 and 5.0 mV, respectively. A similar trend for particle size and zeta potential was also observed for the DOPE containing formulation group, however relatively large LNP diameters were reported for these preparations.

3.2. Encapsulation of siRNA in lipid nanoparticles

The encapsulation of siRNA in the various nanoparticle preparation types was determined using Ribogreen assay. As shown in Table 2, free siRNA (not encapsulated or associated with the nanoparticles) was observed in the DOPC (100%) formulation. Free siRNA was <LLOD (lowest limit of detection) for all formulations containing DOTAP, including those preparations for when a relatively high percentage of PEG was employed. For the DOPC-based formulations the encapsulation of siRNA decreased slightly compared to DOPC/DOTAP (50/50) when the PEG content increased from 0 to 10 mol%. To evaluate if the decreased encapsulation was associated with the electronegative charge from the phosphate group in DOPE-PEG_{2000}, ten percent of DSG-PEG_{2000} was employed (to replace DOPE-PEG_{2000}) in the DOPC/DOTAP formulation. We observed no increase in the total amount of encapsulated siRNA when compared to DOPE-PEG_{2000}, suggesting that the decreased encapsulation was not electronegative charge-mediated. A similar trend was also observed with the DOPE-based formulations (Table 2).

Table 1
Characterization of lipid nanoparticles.

Composition	Ratio	Particle size (nm)	Zeta potential (mV)
DOPC	100	178 ± 17.6	2 ± 4.1
DOPC/DOTAP	50/50	149 ± 14.3	45 ± 3.7
DOPC/DOTAP/DOPE-PEG_{2000}	48/50/2	113 ± 7.2	30 ± 3.9
	45/50/5	105 ± 4.5	23 ± 2.6
	40/50/10	102 ± 6.9	5 ± 2.4
DOPE	100	341 ± 41.3	−3 ± 5.3
DOPE/DOTAP	50/50	217 ± 21.8	43 ± 7.7
DOPE/DOTAP/DOPE-PEG_{2000}	48/50/2	118 ± 10.5	31 ± 4.9
	45/50/5	113 ± 8.3	21 ± 4.6
	40/50/10	104 ± 2.3	−1.1 ± 4.7

3.3. LNP characterization based on density

LNPs containing siRNA/DOPC/DOTAP and different percentage of DOPE-PEG_{2000} were ultracentrifuged at 120,000 rpm for 2 h in continuous glucose gradient. Empty liposomes containing DOPC/DOTAP/DOPE-PEG_{2000} (45/50/5, mol%) were employed as a control. All empty particles remained at the very top of the glucose gradient following ultracentrifugation. However, for all siRNA containing LNPs, two bands were observed in the glucose gradient. One light band was at the top of the centrifuge tube representing particles lighter than PBS, the other thick band settled at approximately 4% glucose. Therefore, three fractions containing the top band, the bottom band and the gradient between the two bands from each tube were collected and analyzed. The size measurements did not reveal significant differences among the nanoparticles. All LNPs ranged between 95 and 115 nm in size (Table 3). However, Ribogreen analysis revealed a rather significant difference in siRNA content among the three fractions, and the majority of siRNA was associated with the bottom band regardless of the percentage of DOPE-PEG_{2000} employed (Table 3).

3.4. LNP toxicity study

Endothelial cell lines have long been employed as *in vitro* models for studying tumor angiogenesis and pathophysiologic function [18,19]. However, unlike cancer cells that grow uncontrollably, and mutate to survive in response to a toxic environment, healthy endothelial cells can be highly susceptible to lipid toxicity. Therefore, toxicity/safety studies of lipid nanoparticles were performed with the use of sulforhodamine B cytotoxicity assay on a variety of endothelial cell lines (Fig. 1A–F). The DOPC/DOTAP particles (which did not contain PEG) exhibited severe cellular toxicity at concentrations as low as 10 μM, and a sharp decrease in cell viability was observed with both HMEC-1 (88 ± 10.9%) and HUVEC (87 ± 11.9%) cells. A similar toxic effect was observed with MS1-VEGF cells at a higher concentration of 50 μM (82 ± 4.3%). Overall, an increase in PEG content (from 2 to 10 mol%) of DOPC nanoparticles decreased the level of cellular toxicity for the cationic nanoparticles. Similar results were observed with DOPE-based nanoparticles (Fig. 1D–F).

Table 2
Evaluation of siRNA encapsulation in LNP.

Formulation composition	Ratio (mole)	%siRNA (Free)	%siRNA (Associated)	%siRNA (Encapsulated)
DOPC	100	64.3	16.1	19.6
DOPC/DOTAP	50/50	<LLOD	17.8	82.2
DOPC/DOTAP/DOPE-PEG_{2000}	48/50/2	<LLOD	19.9	80.1
DOPC/DOTAP/DOPE-PEG_{2000}	45/50/5	<LLOD	21.3	78.7
DOPC/DOTAP/DOPE-PEG_{2000}	40/50/10	<LLOD	27.0	73.0
DOPC/DOTAP/DSG-PEG_{2000}	40/50/10	<LLOD	25.7	74.3
DOPE	100	78.1	9.7	12.2
DOPE/DOTAP	50/50	<LLOD	26.1	73.9
DOPE/DOTAP/DOPE-PEG_{2000}	48/50/2	<LLOD	20.7	79.3
DOPE/DOTAP/DOPE-PEG_{2000}	45/50/5	<LLOD	24.9	75.1
DOPE/DOTAP/DOPE-PEG_{2000}	40/50/10	<LLOD	29.8	70.2

Table 3
LNP separation and characterization based on density.

	Sample	Size (nm)	PDI	Encapsulation (%)	Total RNA content (ug)	Payload distribution (%)
DOPC/DOTAP (50/50)	Parental	104.4	0.12	81	1.73	100.00
	Fraction 1 (Top)	102.4	0.09	85	0.03	1.82
	Fraction 2 (Middle)	97.7	0.33	<LLOD	<LLOD	N/A
	Fraction 3 (Bottom)	100.0	0.12	78	1.47	84.80
DOPC/DOTAP/DOPE-PEG$_{2000}$ (48/50/2)	Parental	99.2	0.09	79	2.12	100.00
	Fraction 1 (Top)	106.8	0.08	85	0.05	2.28
	Fraction 2 (Middle)	115.8	0.18	75	0.03	1.32
	Fraction 3 (Bottom)	103.8	0.11	78	1.69	79.89
DOPC/DOTAP/DOPE-PEG$_{2000}$ (45/50/5)	Parental	97.5	0.11	78	1.66	100.00
	Fraction 1 (Top)	100.0	0.12	78	0.20	12.05
	Fraction 2 (Middle)	97.7	0.22	67	0.06	3.43
	Fraction 2 (Bottom)	104.5	0.13	76	1.34	80.92
DOPC/DOTAP/DOPE-PEG$_{2000}$ (40/50/10)	Parental	95.6	0.11	75	1.82	100.00
	Fraction 1 (Top)	99.7	0.13	60	0.36	19.96
	Fraction 2 (Middle)	101.0	0.14	85	0.02	0.86
	Fraction 3 (Bottom)	105.9	0.12	76	1.06	58.38

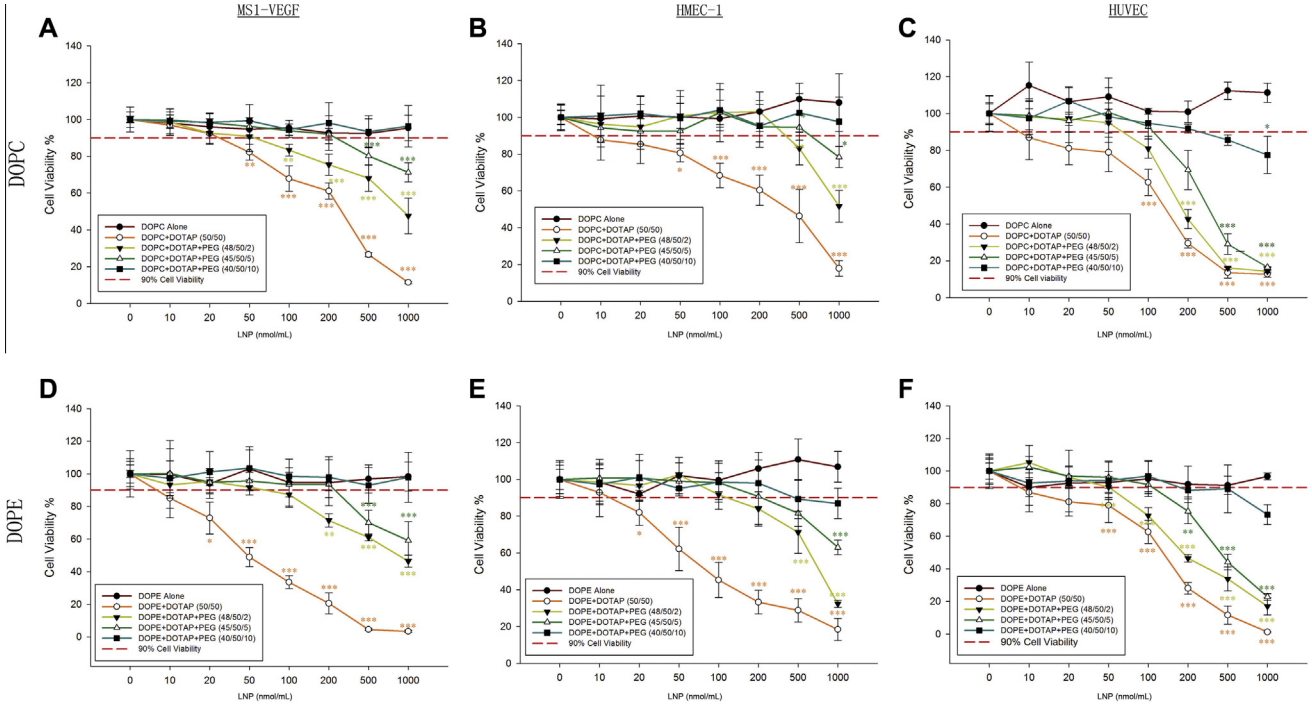

Fig. 1. Cell viability as a function of LNP composition. Dotted lines (···) were used to indicate 90% of cell viability. Results were presented as mean ± s.d. (n = 6).

3.5. Cellular uptake of siRNA in vitro

Polyethylene glycol is frequently used to formulate nanoparticles to increase the *in vivo* half-life of drug-loaded nanoparticles. PEG limits the interaction of drug carrier molecules with insoluble blood proteins that would otherwise accelerate the clearance of nanoparticles. This is a beneficial property of PEG for siRNA delivery provided the role of DOTAP is not overshadowed by the presence of PEG. We thus seek to establish what affect the long chain polymer, when employed in combination with DOTAP, has on the cellular uptake of siRNA. FACS analysis was employed to investigate the uptake of siRNA by cells. Compared to the baseline control, no cellular uptake of siRNA was observed in the DOPE-siRNA group (Fig. 2B). We did observe a modest amount of cellular uptake in the DOPC-siRNA group (Fig. 2A). In general, these electroneutral nanoparticles are not well suited to deliver siRNA to target cells. However, following the inclusion of DOTAP in the LNPs (DOPC/DOTAP), we observed a dramatic right shift of the peak from the baseline cell control. Interestingly, this level of cellular uptake was sustained following the inclusion of a modest amount of PEG (2% or 5%). However, when 10 mol% of PEG was used the uptake of siRNA by MS1-VEGF cells was similar to the delivery of naked siRNA. Similar results were also observed in DOPE-based LNP formulations. The inclusion of the relatively high PEG content lowered the cationic zeta potential, and natural affinity of the siRNA-LNPs for the target cell. The ratio of DOTAP to PEG should thus be optimized to achieve desired results.

3.6. Growth inhibition by KSP siRNA

KSP siRNA has been chemically modified by introducing a phosphorothioate (P = S) backbone linkage at the 3′ end for exonuclease resistance and 2′ modifications (2′-OMe) to mitigate immunostimulatory properties. These chemical modifications have no

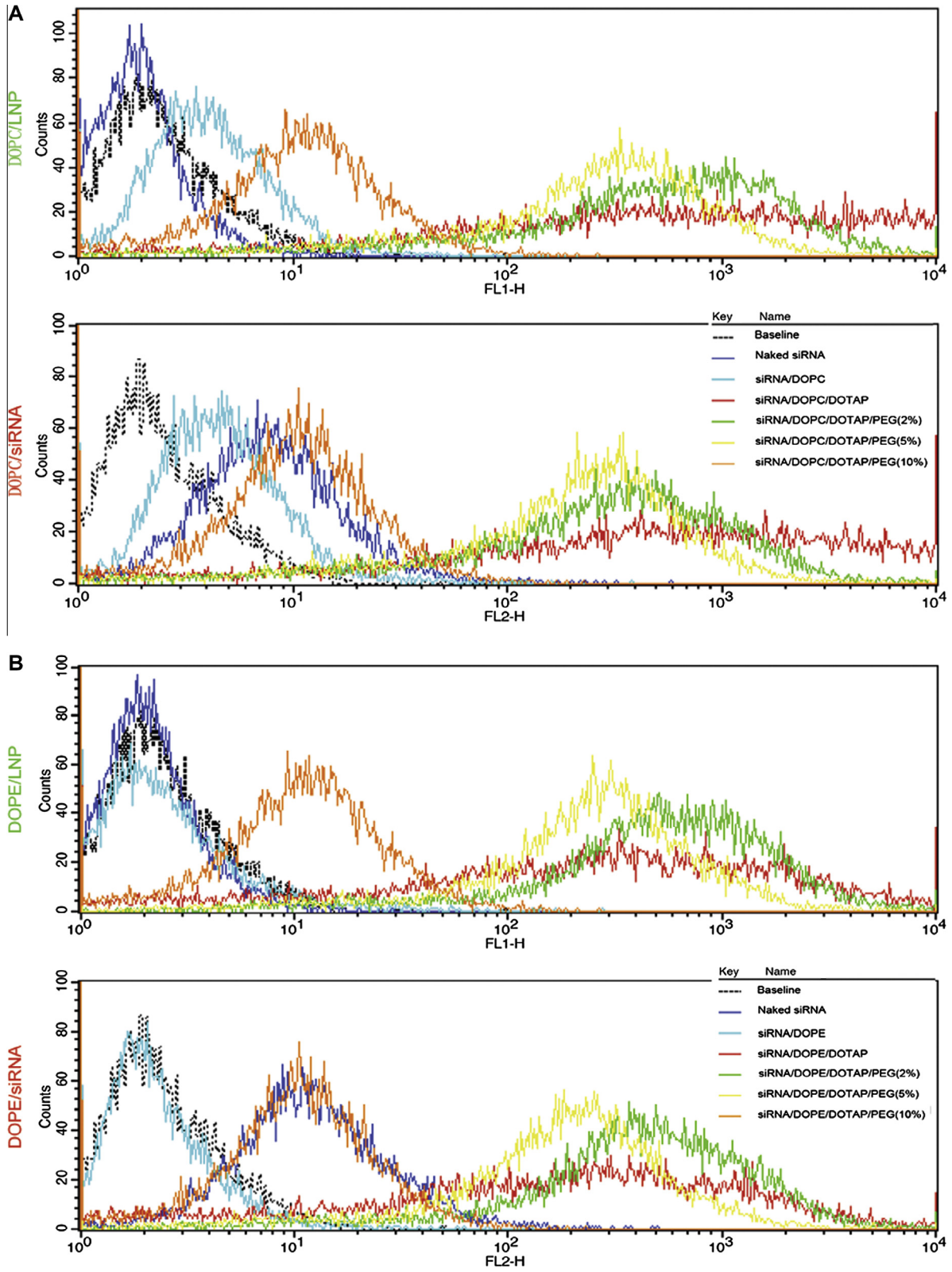

Fig. 2. Cellular uptake as a function of PEG percentage. FL1-H and FL2-H indicate channels employed to monitor the uptake of LNP and siRNA by MS1-VEGF cells, respectively. Black dotted lines indicate MS1-VEGF cells alone as baseline. Dark blue lines represent naked siRNA. Light blue lines indicate the uptake of siRNA or electroneutral LNPs. Red lines indicate siRNA formulated using DOTAP particles without PEGylation. Green, yellow and orange lines indicate LNPs with 2, 5, 10 mol percent of DOPE-PEG_{2000}, respectively. (A) LNP and siRNA uptake on DOPC based formulations; (B) LNP and siRNA uptake on DOPE based formulations. (For interpretation of the references to colour in this figure legend, the reader is referred to the web version of this article.)

effect on the overall charge of KSP siRNA [20]. MS1-VEGF cells were exposed to an increased amount of KSP siRNA, or control siRNA, formulated with LNPs with different compositions for 48 h prior to SRB cytotoxicity assay and analysis. LNPs loaded with control siRNA showed a marginal inhibitory effect on cell proliferation (Fig. 3A). However, LNPs loaded with KSP siRNA demonstrated

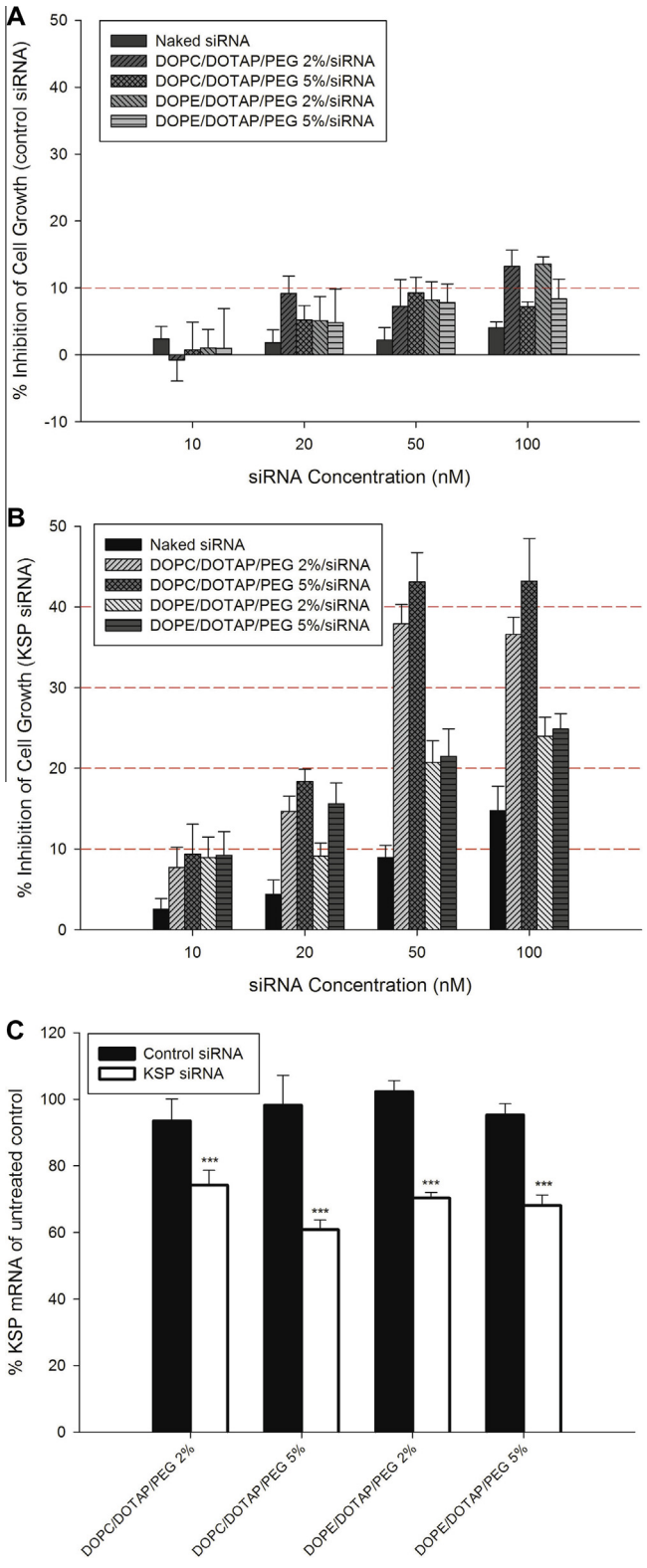

Fig. 3. Growth inhibition of endothelial cells by knocking-down KSP mRNA using KSP siRNA-loaded LNPs. (A and B) Growth inhibition was measured using SRB assay after 48-h exposure to LNPs. Results were presented as mean ± s.d. (n = 8). (C) Cells were seeded at 5 * 10^5 cells per ml in 6-well plates for 24 h before being exposed to KSP siRNA or control siRNA. After 48-h incubation, total RNA was extracted, transcribed and amplified. Beta-actin was used as internal control and all data were converted to the percentage of the KSP mRNA from untreated cells. Results were presented as mean ± s.d. (n = 8) and analyzed using paired t-test.

concentration-dependent growth inhibition (Fig. 3B), suggesting the potential of silencing KSP as a novel anti-angiogenic therapeutic strategy against cancer. The findings confirm that the growth inhibition was a result of a direct knock-down in the KSP mRNA expression, as confirmed by real time RT-PCR (Fig. 3C).

4. Discussion

Liposomes are promising drug carrier molecules given their success with delivering various chemotherapeutic agents to tumors through the EPR (enhanced permeability and retention) effect [21]. The liposome varieties typically used for this purpose possess either an overall negative or nominally electroneutral surface charge (zeta potential) through PEGylation. For this reason, they often lack the ability to facilitate drug entry into endothelial cells, and are thus not normally considered a first choice delivery vehicle for selective tumor vascular targeting.

In addition to interstitial tumor targeting strategies, cationic liposomes have also been used to deliver drug agents to the tumor vasculature. Interaction of cationic liposome therapeutics with tumor vessels in preclinical models frequently results in the suppression and/or the complete eradication of tumor growth [4]. Moreover, clinical trial studies strongly support the use of cationic liposomes to treat human metastatic breast and pancreatic cancer diseases [4].

To improve the encapsulation, small molecules can be loaded into liposomes more actively using transient ion pairs or pH gradient [22,23]. However, a typical 21mer siRNA (MW ~13 k) is mostly formulated in lipid particles through spontaneous particle formation, such as thin film hydration method, detergent dialysis and ethanol dilution [24]. The high free siRNA content and low encapsulation rate observed with DOPC and DOPE lipid particles can be due to the lack of interaction between lipids and siRNA as well as the limited volume of aqueous content engulfed by lipid bilayers. However, it is hard to explain the high encapsulation efficiency of siRNA (much higher than 50%) observed with cationic lipid particles if passive encapsulation is the only mechanism involved. Therefore, we speculate that the formulation of siRNA-containing LNPs includes two stages. First, the cationic lipids interact with oligonucleotides to form complexes through charge interaction. Next, other lipids are gradually deposited onto the complex to form particles until the surface is stabilized either by charge repulsion or with sufficient coverage of PEG (Fig. 4). The decreased encapsulation observed with 10 percent of PEGylation could be due to either the formation of empty particles with RNA associated on the outer surface, or the excess amount of PEG preventing further lipid deposition on the complex/particles prematurely. Results from the density gradient separation revealed the presence of two distinct populations. The major population which contains the majority of siRNA exhibited density similar to 4% glucose, while similar to empty particles, the minor fraction associated with less amount of siRNA was lighter than PBS. These results indicate the formation of solid lipid/RNA nanoparticles in the presence of RNA. It has also been shown that siRNA containing LNPs prepared using the microfluidic mixing method exhibited an electron-dense core [25], suggesting the interaction between cationic lipids and siRNA may play an important role in the particle formation which is different from the passive theories of accumulation. Still, further analysis is needed to confirm if the minor fraction contains siRNA sandwiched between empty particles, or whether the fractions contain partially loaded particles with siRNA encapsulated inside or superficially associated with the lipid membrane.

In this study, a relatively high percentage of polyethylene glycol in LNPs prevented efficient cellular uptake/binding *in vitro*. This is

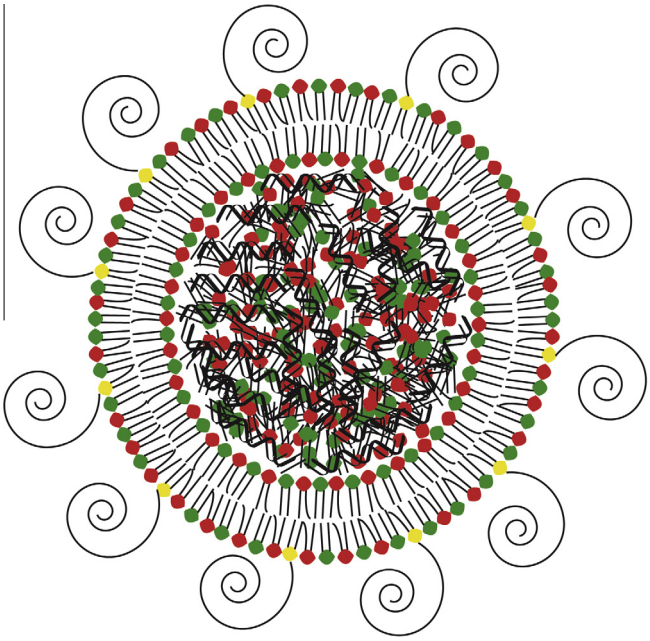

Fig. 4. Schematic of siRNA/LNP complex.

not surprising given that PEGylation has long been used to prolong the circulating time of particles *in vivo,* and is not frequently employed to facilitate cellular uptake of therapeutics. To overcome this intrinsic dilemma, PEG lipids with shorter anchors or environment-sensitive properties are preferred [13,26,27].

Kinesin spindle protein (KSP) is a promising target for cancer treatment not only due to its ability to mediate the segregation of centrosomes during mitosis, but given that there is little, if any, KSP expression in non-mitotic cells [14,15,28]. Intravenous delivery of KSP siRNA in SNALP has been shown to extend the survival time of mice-bearing hepatic Neuro2a tumors [17]. The data show significant growth inhibition of transformed endothelial cells when KSP siRNA was delivered using LNPs, suggesting the potential for targeting KSP as an effective approach in anti-angiogenic therapy. For this reason, subsequent *in vivo* investigations are necessary to determine possible clinical relevance.

Acknowledgments

The authors thank Dr. Michail Sitkovsky, PhD., from the Department of Pharmaceutical Sciences, Northeastern University (NU), Boston, MA for kindly providing access to the FACS and Real-Time PCR systems. We thank Alnylam Pharmaceuticals, Cambridge, MA and Dr. Dinah Sah, PhD., for generously providing KSP (and control) siRNA and for offering valuable suggestions, respectively. The manuscript represents work submitted in partial fulfillment of Doctoral degree at NU for Dr. Bo Ying, PhD. The study was funded in part by the National Science Foundation CMMI Grant No. 1232339 for R.B.C.

References

[1] J. Folkman, Tumor angiogenesis: therapeutic implications, N. Engl. J. Med. 285 (1971) 1182–1186.
[2] J. Denekamp, The tumour microcirculation as a target in cancer therapy: a clearer perspective, Eur. J. Clin. Invest. 29 (1999) 733–736.
[3] J. Folkman, Angiogenesis: an organizing principle for drug discovery?, Nat Rev. Drug Discov. 6 (2007) 273–286.
[4] R.B. Campbell, Tumor physiology and delivery of nanopharmaceuticals, Anticancer Agents Med. Chem. 6 (2006) 503–512.
[5] S. Dabbas, R.R. Kaushik, S. Dandamudi, G.M. Kuesters, R.B. Campbell, Importance of the liposomal cationic lipid content and type in tumor vascular targeting: physicochemical characterization and *in vitro* studies using human primary and transformed endothelial cells, Endothelium 15 (2008) 189–201.
[6] G. Thurston, J.W. McLean, M. Rizen, P. Baluk, A. Haskell, T.J. Murphy, D. Hanahan, D.M. McDonald, Cationic liposomes target angiogenic endothelial cells in tumors and chronic inflammation in mice, J. Clin. Invest. 101 (1998) 1401–1413.
[7] K.A. Whitehead, R. Langer, D.G. Anderson, Knocking down barriers: advances in siRNA delivery, Nat. Rev. Drug Discov. 8 (2009) 129–138.
[8] A. Fire, S. Xu, M.K. Montgomery, S.A. Kostas, S.E. Driver, C.C. Mello, Potent and specific genetic interference by double-stranded RNA in *Caenorhabditis elegans*, Nature 391 (1998) 806–811.
[9] N.J. Caplen, E. Kinrade, F. Sorgi, X. Gao, D. Gruenert, D. Geddes, C. Coutelle, L. Huang, E.W. Alton, R. Williamson, *In vitro* liposome-mediated DNA transfection of epithelial cell lines using the cationic liposome DC-Chol/DOPE, Gene Ther. 2 (1995) 603–613.
[10] K.M. Gaensler, G. Tu, S. Bruch, D. Liggitt, G.S. Lipshutz, A. Metkus, M. Harrison, T.D. Heath, R.J. Debs, Fetal gene transfer by transuterine injection of cationic liposome-DNA complexes, Nat. Biotechnol. 17 (1999) 1188–1192.
[11] D.L. Reimer, S. Kong, M. Monck, J. Wyles, P. Tam, E.K. Wasan, M.B. Bally, Liposomal lipid and plasmid DNA delivery to B16/BL6 tumors after intraperitoneal administration of cationic liposome DNA aggregates, J. Pharmacol. Exp. Ther. 289 (1999) 807–815.
[12] D.J. Stephan, Z.Y. Yang, H. San, R.D. Simari, C.J. Wheeler, P.L. Felgner, D. Gordon, G.J. Nabel, E.G. Nabel, A new cationic liposome DNA complex enhances the efficiency of arterial gene transfer in vivo, Hum. Gene Ther. 7 (1996) 1803–1812.
[13] S.C. Semple, A. Akinc, J. Chen, A.P. Sandhu, B.L. Mui, C.K. Cho, D.W. Sah, D. Stebbing, E.J. Crosley, E. Yaworski, I.M. Hafez, J.R. Dorkin, J. Qin, K. Lam, K.G. Rajeev, K.F. Wong, L.B. Jeffs, L. Nechev, M.L. Eisenhardt, M. Jayaraman, M. Kazem, M.A. Maier, M. Srinivasulu, M.J. Weinstein, Q. Chen, R. Alvarez, S.A. Barros, S. De, S.K. Klimuk, T. Borland, V. Kosovrasti, W.L. Cantley, Y.K. Tam, M. Manoharan, M.A. Ciufolini, M.A. Tracy, A. de Fougerolles, I. MacLachlan, P.R. Cullis, T.D. Madden, M.J. Hope, Rational design of cationic lipids for siRNA delivery, Nat. Biotechnol. 28 (2010) 172–176.
[14] D. Huszar, M.E. Theoclitou, J. Skolnik, R. Herbst, Kinesin motor proteins as targets for cancer therapy, Cancer Metastasis Rev. 28 (2009) 197–208.
[15] V. Sarli, A. Giannis, Targeting the kinesin spindle protein: basic principles and clinical implications, Clin. Cancer Res. 14 (2008) 7583–7587.
[16] W. Tao, V.J. South, Y. Zhang, J.P. Davide, L. Farrell, N.E. Kohl, L. Sepp-Lorenzino, R.B. Lobell, Induction of apoptosis by an inhibitor of the mitotic kinesin KSP requires both activation of the spindle assembly checkpoint and mitotic slippage, Cancer Cell 8 (2005) 49–59.
[17] A.D. Judge, M. Robbins, I. Tavakoli, J. Levi, L. Hu, A. Fronda, E. Ambegia, K. McClintock, I. MacLachlan, Confirming the RNAi-mediated mechanism of action of siRNA-based cancer therapeutics in mice, J. Clin. Invest. 119 (2009) 661–673.
[18] F. Goto, K. Goto, K. Weindel, J. Folkman, Synergistic effects of vascular endothelial growth factor and basic fibroblast growth factor on the proliferation and cord formation of bovine capillary endothelial cells within collagen gels, Lab. Invest. 69 (1993) 508–517.
[19] M.A. Gimbrone Jr., R.S. Cotran, J. Folkman, Human vascular endothelial cells in culture. Growth and DNA synthesis, J. Cell Biol. 60 (1974) 673–684.
[20] M. Manoharan, RNA interference and chemically modified small interfering RNAs, Curr. Opin. Chem. Biol. 8 (2004) 570–579.
[21] V.P. Torchilin, Recent advances with liposomes as pharmaceutical carriers, Nat. Rev. Drug Discov. 4 (2005) 145–160.
[22] S.A. Abraham, K. Edwards, G. Karlsson, S. MacIntosh, L.D. Mayer, C. McKenzie, M.B. Bally, Formation of transition metal-doxorubicin complexes inside liposomes, Biochim. Biophys. Acta 1565 (2002) 41–54.
[23] L.D. Mayer, L.C. Tai, M.B. Bally, G.N. Mitilenes, R.S. Ginsberg, P.R. Cullis, Characterization of liposomal systems containing doxorubicin entrapped in response to pH gradients, Biochim. Biophys. Acta 1025 (1990) 143–151.
[24] L.B. Jeffs, L.R. Palmer, E.G. Ambegia, C. Giesbrecht, S. Ewanick, I. MacLachlan, A scalable, extrusion-free method for efficient liposomal encapsulation of plasmid DNA, Pharm. Res. 22 (2005) 362–372.
[25] A.K. Leung, I.M. Hafez, S. Baoukina, N.M. Belliveau, I.V. Zhigaltsev, E. Afshinmanesh, D.P. Tieleman, C.L. Hansen, M.J. Hope, P.R. Cullis, Lipid nanoparticles containing siRNA synthesized by microfluidic mixing exhibit an electron-dense nanostructured core, J. Phys. Chem. C: Nanomater. Interfaces 116 (2012) 18440–18450.
[26] D. Chen, W. Liu, Y. Shen, H. Mu, Y. Zhang, R. Liang, A. Wang, K. Sun, F. Fu, Effects of a novel pH-sensitive liposome with cleavable esterase-catalyzed and pH-responsive double smart mPEG lipid derivative on ABC phenomenon, Int. J. Nanomed. 6 (2011) 2053–2061.
[27] X. Guo, F.C. Szoka Jr., Steric stabilization of fusogenic liposomes by a low-pH sensitive PEG–diortho ester–lipid conjugate, Bioconjug. Chem. 12 (2001) 291–300.
[28] S.D. Knight, C.A. Parrish, Recent progress in the identification and clinical evaluation of inhibitors of the mitotic kinesin KSP, Curr. Top. Med. Chem. 8 (2008) 888–904.